Effect of Dynamic Loading on the Transport of Solutes into Agarose Hydrogels

Nadeen O. Chahine,[†] Michael B. Albro,[‡] Eric G. Lima,[§] Victoria I. Wei,[‡] Christopher R. Dubois,[§] Clark T. Hung,[§] and Gerard A. Ateshian[‡*]

[†]Biomechanics & Bioengineering Research Laboratory, Feinstein Institute for Medical Research, North Shore Long Island Jewish Health System, Manhasset, New York; and [‡]Musculoskeletal Biomechanics Laboratory, [§]Cellular Engineering Laboratory, Department of Biomedical Engineering, Columbia University, New York, New York

ABSTRACT In functional tissue engineering, the application of dynamic loading has been shown to improve the mechanical properties of chondrocyte-seeded agarose hydrogels relative to unloaded free swelling controls. The goal of this study is to determine the effect of dynamic loading on the transport of nutrients in tissue-engineered constructs. To eliminate confounding effects, such as nutrient consumption in cell-laden disks, this study examines the response of solute transport due to loading using a model system of acellular agarose disks and dextran in phosphate-buffered saline (3 and 70 kDa). An examination of the passive diffusion response of dextran in agarose confirms the applicability of Fick's law of diffusion in describing the behavior of dextran. Under static loading, the application of compressive strain decreased the total interstitial volume available for the 70 kDa dextran, compared to free swelling. Dynamic loading significantly enhanced the rate of solute uptake into agarose disks, relative to static loading. Moreover, the steady-state concentration under dynamic loading was found to be significantly greater than under static loading, for larger-molecular-mass dextran (70 kDa). This experimental finding confirms recent theoretical predictions that mechanical pumping of a porous tissue may actively transport solutes into the disk against their concentration gradient. The results of this study support the hypothesis that the application of dynamic loading in the presence of growth factors of large molecular weight may result in both a mechanically and chemically stimulating environment for tissue growth.

INTRODUCTION

Articular cartilage is a dense white tissue that lines the bony surfaces of diarthrodial joints and transmits loads during joint motion. Adult articular cartilage is an avascular tissue, composed of water and a dense extracellular matrix. Nutrient supply to chondrocytes occurs through transport from surrounding tissues and structures. In immature joints, nutrients are supplied to the tissue through diffusion from the subchondral bone and the synovial fluid. However, after maturation, the fusion of the subchondral plate limits diffusion from the underlying bone, thus nutrients diffuse into the tissue primarily from the synovial fluid via the articular surface. Transport also plays a fundamental role in the removal of waste products of chondrocytes (1).

Mechanical loading of cartilage has been shown to be efficacious and necessary for the maintenance of normal metabolic activities of chondrocytes, where biosynthetic responses are coupled to the sensation of the mechanical signal. Moreover, these loading protocols are also thought to alter the transport behavior of the extracellular matrix. Static loading has been shown to decrease the diffusivity of solutes into tissue explants (2–4), whereas dynamic loading has been shown to enhance the efflux of large solutes out of cartilage explants (4–6). Additionally, studies have indicated that dynamic loading enhances the rate of uptake of growth factors into the cartilage matrix (7). Consequently, there are at least two major driving forces modulating the metabolic responses of chondrocytes in tissues. It is uncertain whether the loading-induced metabolic responses are due to changes in the nutritional supply to the cells, or the chondrocytes are responding to the direct sensation of mechanical signals, although both mechanisms are likely to play a role.

In functional tissue engineering, the application of dynamic loading (DL) has also been shown to improve the mechanical properties and biochemical content of chondrocyte-seeded agarose hydrogels relative to unloaded free swelling (FS) controls (8–10). Possible mechanisms leading to the cartilaginous growth in this hydrogel scaffold are likely to be similar to the mechanisms leading to metabolic changes in cartilage.

The objective of this study is to determine the effect of dynamic loading on the transport of solutes in tissue-engineered constructs. We examine the response of solute transport due to loading using a model system of acellular agarose disks and dextran in phosphate-buffered saline (PBS). Changes in nutrient supply are investigated by examining the behavior of dextran conjugated with Texas Red, resulting in an inert, neutral, fluorescently detectable solute. The behavior of 3 kDa and 70 kDa dextran are examined, two molecular masses comparable to growth factors important in chondrocyte metabolism (IGF-1, 8 kDa; TGF-β1, 25 kDa). Preliminarily, the suitability of Fickian diffusion analysis is examined for modeling the transport of chainlike dextran molecules in agarose. In addition, the effect of compressive strain-dependence on dextran partition coefficient is examined.

Submitted July 29, 2008, and accepted for publication May 20, 2009.

*Correspondence: ateshian@columbia.edu

Editor: Elliot L. Elson.

0006-3495/09/08/0968/8 $2.00

doi: 10.1016/j.bpj.2009.05.047

MATERIALS AND METHODS

Acellular type-VII low melting agarose (Sigma, St. Louis, MO) was dissolved in 100 mL of phosphate-buffered saline (PBS) at a concentration of 2% w/v. The mixture was autoclaved to ensure good solubilization, allowed to cool to room temperature, then remelted in the microwave (no more than twice) before casting between two glass plates. Slabs were gelled at room temperature for 30 min, then transferred and stored in sterile PBS until use. Agarose disks were used in this study within 7–10 days of casting to eliminate any long-term degradation of the hydrogel integrity.

Study 1: analysis of Fickian diffusion

Cylindrical disks, ∅1.5-mm × 1.5-mm thick, were prepared from the agarose slab using a biopsy punch. Disks were loaded under unconfined static compression in a custom loading device sitting on the stage of a confocal microscope (Fig. 1). Samples were placed in the center of a testing chamber, consisting of a quartz-glass bottom reinforced with an aluminum base. A static compressive offset, of 10% strain, was imposed using a platen actuated with a micrometer attached to a translating stage. Disks were exposed to a bathing solution of PBS + dextran conjugated with Texas Red (70 kDa, 0.5 mg/mL; Molecular Probes, Eugene, OR). The bathing solution was circulated with a peristaltic pump (30 mL/min, IPC model; Ismatec, Glattbrugg, Switzerland) through two portals located in the lid of the testing chamber.

Confocal microscopy was used to image the disk's circular cross section and the surrounding bath over time (Olympus IX70 and FluoView Imaging System; Olympus, Melville, NY). The relatively small diameter of the disk made it possible to image more than half of the disk within a single field of view. A region of interest, consisting of one-half of the disk with its surrounding bathing solution, was imaged every 15 min at 10–20 μm away from the surface of the disk using a 10× objective (resolution = 1.34 μm/pixel). The fluorescence intensity of the solute in the disk over time was analyzed using MATLAB (The MathWorks, Natick, MA). The solute concentration in the disk, $c(r,t)$, normalized to the bathing concentration, c^*, was calculated as a ratio of the intensity in the disk, $I(r,t)$, to that in the bathing solution, I^*,

$$\frac{c(r,t)}{c^*} = \frac{1}{\varphi^w}\frac{I(r,t)}{I^*}, \tag{1}$$

with φ^w representing the volume fraction of water (porosity) of the agarose disks. Thus, the concentration $c(r,t)$ represents the number of moles of solute per volume of solvent in the hydrogel.

The average solute concentration over time, $\bar{c}(t)$, was determined by computing the average concentration of the solute at all positions within the disk for each time point. The spatio-temporal response, $c(r,t)$, was computed at even increments along the radius a of the sample for each time point ($\hat{r} = r/a = 0, 0.25, 0.5, 0.75, 1$). Both computations were dependent on accurate assessment of the disk boundary. In each image, 3–5 points were identified along the disk-bath interface, and a semicircular region representing the disk was identified by locating the common center of curvature of these points along the edge. Consequently, all position-dependent analyses were computed relative to the identified center of the disk in each image, $\hat{r} = 0$.

Study 2: effect of loading

Experimental setup

Acellular agarose disks (2% w/v) were prepared (∅5 mm × 2.3 mm thick), and constructs were divided into three equal groups ($n = 8$ per group): free swelling control (FS), static loading (SL), and dynamic loading (DL), and placed in the center of a custom-loading dish (Fig. 2, *inset*). A 0.5-mm-thick template, of 3% type IB agarose, was cast in the base of each loading dish, and each disk was placed in the center of a ∅6.35 mm recess. Next, a 10-mL bathing solution of PBS and dextran conjugated with Texas Red (0.5 mg/mL; Molecular Probes) was added to each dish. In this study, the behavior of 3 kDa and 70 kDa dextran solutions was examined. During the experiment, the bathing solution in each dish was circulated using a peristaltic pump (40 mL/min, IPC model; Ismatec) to maintain a well-stirred environment and eliminate the presence of unstirred boundary layers.

Loading protocol

Once exposed to the bathing solution, each testing group was maintained in a light-sensitive environment at 37°C. Agarose constructs were loaded up to 24 h (10 min, 30 min, 1 h, 3 h, 6 h, 12 h, and 24 h) in a custom unconfined compression-loading device under impermeable platens (Fig. 2). The device consisted of a lead screw driving deformation to the bottom loading platen via a rotary stepper motor. A 10% static offset was applied to both the SL and DL loading groups. An additional dynamic strain of 10% was applied to the DL samples at 1 Hz frequency. The FS group was maintained in the same environment as the loaded groups and served as the free-swelling control.

Solute content measurement

Upon completion of loading, several aliquots of the bathing solution were collected and stored for content analysis. All disks were removed from the bathing solution, excess solution was blotted, and each disk was resuspended in 200 μL of PBS. Each disk was then pulverized and stored at 4°C for 48 h to allow the solute molecules to diffuse out of the gel. The gel/solute mixture was then centrifuged (14,000 rpm for 30 min at 10°C, Eppendorf microcentrifuge 5417R; Fisher Scientific, Pittsburgh, PA), and the supernatant containing the fluorescently labeled solute was extracted. The solute concentration was measured using a fluorescent plate reader at

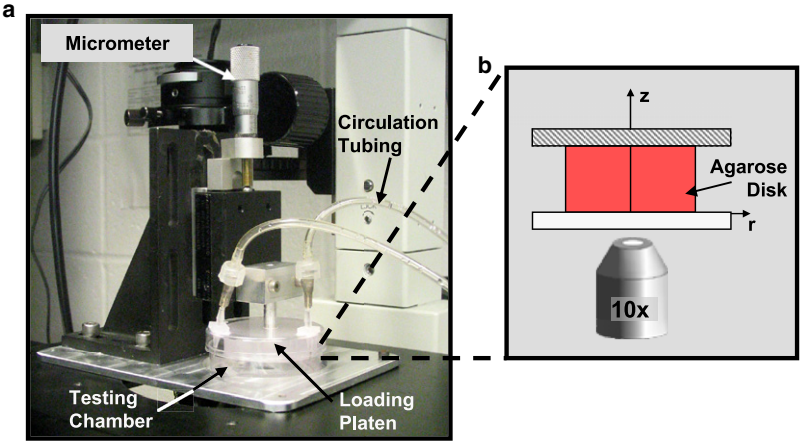

FIGURE 1 Microscope-mounted loading device utilized in examining the spatio-temporal diffusion behavior of dextran in agarose (Study 1). Agarose disks were placed in the testing chamber, static compression was applied with the loading platen and micrometer from above, and dextran solution was circulated using peristaltic pump (not shown). Images of disk cross section with surrounding dextran solution were acquired using confocal microscope over time.

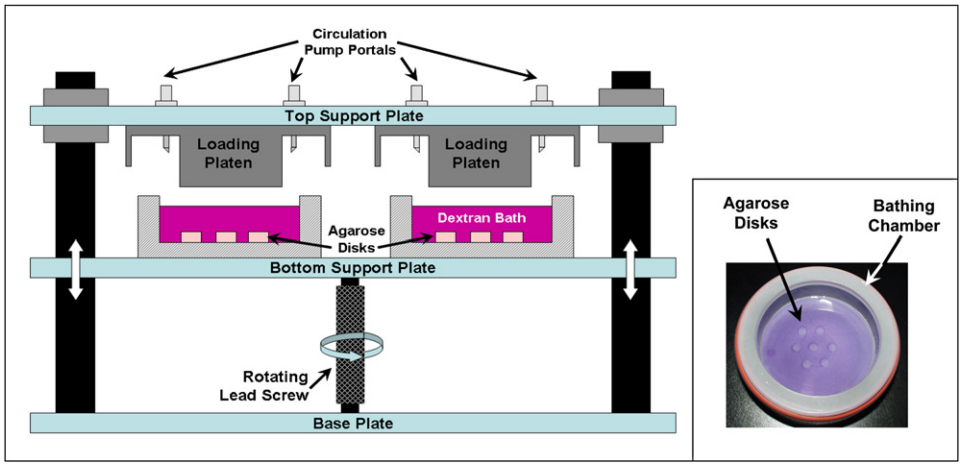

FIGURE 2 Loading device utilized in applying static and dynamic loading to agarose disks in the presence of dextran solutions at 37°C. Agarose disks were placed in the center of a testing chamber (*inset*), and loaded between two impermeable platens up to 24 h. Tubing for circulating the surrounding bathing solution was inserted into the testing chamber via the portal in the top support plate.

an excitation and emission wavelength of 590 nm and 617 nm, respectively (SpectraFluor Plus; Tecan, Research Triangle Park, NC). A solute-specific standard curve was also assayed with each plate (range: 0–100 μg/mL). The solute concentrations inside the gel were normalized to the bathing solution concentration and are expressed as a concentration ratio.

Study 3: strain-dependent solute uptake

Acellular agarose disks (2% w/v; ∅5 mm × 2.3 mm thick) were loaded to varying static strain magnitudes using a modification of the device described in Study 1, where a reinforced petri dish was used as the base platen in this experiment. A static compressive offset, of 0, 5, 10, 15, or 20% strain was applied at 37°C. Disks were exposed to a bathing solution of 70 kDa Texas-Red conjugated dextran in PBS at 0.5 mg/mL; and circulation was applied using a peristaltic pump (as in Study 1). After 48 h of loading, samples were analyzed using the solute content measurement protocol previously described.

Statistical analysis

In Study 1, a two-way ANOVA was performed to test the effect of molecular mass (3 kDa, 70 kDa) and radial position along the disk $\hat{r} = 0, 0.25, 0.5, 0.75, 1$) on the concentration of dextran. In Study 2, a two-way ANOVA was performed to test the effect of loading configuration (FS, SL, and DL) and time (10 min, 30 min, 1 h, 3 h, 6 h, 12 h, 24 h) on the concentration of dextran in the disks. One-way ANOVA was performed to test the effect of strain magnitude on the equilibrium solute content in Study 3. Tukey-HSD post hoc test was applied for each statistical analysis, with $p < 0.05$ considered statistically significant.

Theoretical analysis

In Study 1, a theoretical analysis of the Fickian diffusion under axisymmetric conditions was performed to model the transport of dextran into a cylindrical disk with radius a, under SL conditions. In this configuration, samples are compressed between two impermeable platens, thus allowing solutes to diffuse into the disk through the radial edges only. The solution for the solute concentration inside the disk, $c(r,t)$, is given by

$$c(r,t) = \kappa c^* \left\{ 1 - 2 \sum_{m=0}^{\infty} \frac{1}{\gamma_m J_1(\gamma_m)} J_0\left(\gamma_m \frac{r}{a}\right) \exp\left(-D \frac{\gamma_m^2}{a^2} t\right) \right\}, \quad (2)$$

where $J_0(\gamma)$ and $J_1(\gamma)$ are zero- and first-order Bessel functions, respectively, and γ_m values are the roots of $J_0(\gamma)$. The value c^* represents the concentration of solutes in the bath, and κ is the partition coefficient, representing the ratio of equilibrium solute concentration inside the disk versus in the surrounding bath, under passive diffusion.

The spatio-temporal response of the solute concentration ratio, $c(r,t)/c^*$, from the microscopy experiments under static loading, were curve-fitted to Eq. 2, yielding a spatially dependent diffusivity (D) and partition coefficient (κ). This analysis was carried out at several positions along the radius ($\hat{r} = r/a = 0, 0.25, 0.5, 0.75, 1$), where $\hat{r} = 0$ and $\hat{r} = 1$ represent the center and edge of the disk, respectively. A comparison of the theoretical versus experimental results for $c(r,t)$ was assessed, and a linear regression analysis was performed to assess the goodness of fit. The parameters, D and κ, extracted from the curve fits are presented in Table 1, as mean ± SD. Significance testing of the curve fit-parameters was carried out using an F-ratio test, with $p < 0.05$ considered statistically significant.

RESULTS

Study 1: analysis of Fickian diffusion

The spatially dependent solute concentration was analyzed at four locations along the radius ($\hat{r} = 0, 0.25, 0.5, 0.75, 1$), and representative responses are shown in Figs. 3 and 4, for 3 and 70 kDa dextran, respectively. The equilibrium solute content of 3 kDa dextran was found to be significantly greater than for 70 kDa dextran (1.02 ± 0.04 for 3 kDa vs. 0.68 ± 0.06 for 70 kDa, $p < 0.05$). Additionally, the equilibrium solute content was found to be comparable near the edge of the disk, in comparison to the center, for both molecular masses (3 kDa: 0.96 ± 0.05 at $\hat{r} = 0$ vs. 1.02 ± 0.04 at $\hat{r} = 0.75$; and 70 kDa: 0.65 ± 0.06 at $\hat{r} = 0$ vs. 0.72 ± 0.06 at $\hat{r} = 0.75$; $p > 0.8$).

The solute content measured experimentally was curve-fitted with the diffusion equation described in Eq. 2, and

TABLE 1 Average diffusivity (D) and partition coefficient (κ) of 3 and 70 kDa dextran under static loading (SL). (n = 3–4 per group)

	$D \times 10^{-11}$ (m^2/s)	κ	R^2
3 kDa	10.21 ± 0.83*	1.016 ± 0.035*	0.996 ± 0.004
70 kDa	2.94 ± 0.41	0.677 ± 0.063	0.991 ± 0.002

The experimental results obtained using the microscopy protocol described in Study 1 were curve-fit with Eq. 2, yielding the reported parameters. Values are reported as mean ± SD.
*Statistical significance between MW groups ($p < 0.05$).

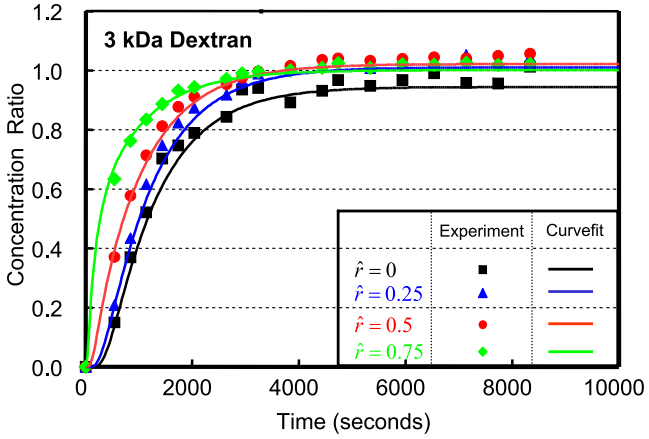

FIGURE 3 Representative spatio-temporal response of 3 kDa dextran measured at even increments along the radius of the sample ($\hat{r} = 0, 0.25, 0.5, 0.75, 1$). Experimental results (indicated by *symbols*) were curve-fitted with Eq. 2, and the resulting fit (*solid lines*) is plotted for comparison.

representative responses are shown in Figs. 3 and 4, for the 3 and 70 kDa dextran, respectively. The resulting diffusivities (D) and partition coefficients (κ) are reported in Table 1, averaged across all radial positions. An excellent agreement was found between the experimental results and the theoretical predictions for both 3 and 70 kDa dextran for all locations along the radius (Figs. 3 and 4), as demonstrated with a near-unity regression coefficient, β (3 kDa: $\beta = 0.982 \pm 0.015$, $R^2 = 0.989 \pm 0.010$; and 70 kDa: $\beta = 0.996 \pm 0.016$, $R^2 = 0.990 \pm 0.007$). Additionally, the 3 kDa dextran exhibited a significantly higher diffusivity and partition coefficient than 70 kDa (D: $10.2 \pm 0.83 \times 10^{-11}$ m^2/s for 3 kDa vs. $2.9 \pm 0.4 \times 10^{-11}$ m^2/s for 70 kDa, $p < 0.0003$; and κ: 1.02 ± 0.04 for 3 kDa vs. 0.68 ± 0.06 for 70 kDa, $p < 0.05$).

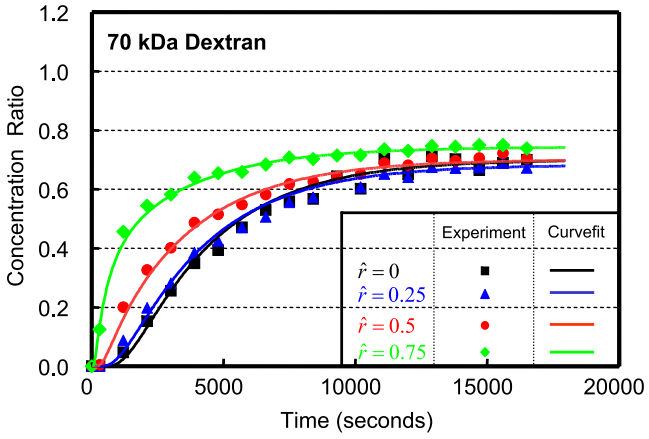

FIGURE 4 Representative spatio-temporal response of 70 kDa dextran measured at even increments along the radius of the sample ($\hat{r} = 0, 0.25, 0.5, 0.75, 1$). Experimental results (indicated by *symbols*) were curve-fitted with Eq. 2, and the resulting fit (*solid lines*) is plotted for comparison.

Study 2: effect of loading

The concentration ratio of both 3 kDa and 70 kDa dextran increased monotonically with time under free swelling (FS) conditions ($p < 0.002$; Fig. 5). Concentration of 3 and 70 kDa dextran reached equilibrium by 12 h of incubation, as demonstrated by insignificant changes in concentration between 12 and 24 h under well-stirred free swelling conditions ($p > 0.95$; Fig. 5). The solute uptake of 3 kDa dextran was $\gg$70 kDa dextran for all time points under 12 h (Fig. 5). The equilibrium solute concentration ratio κ after 24 h of free swelling was found to be 0.97 ± 0.03 and 1.01 ± 0.08 for 3 kDa and 70 kDa dextran, respectively (Fig. 5).

Under static loading (SL), the dextran concentration was diminished in comparison to FS for both molecular masses of dextran (compare Figs. 6 and 7 to Fig. 5). Application of static loading significantly reduced the concentration of 3 kDa dextran after 30 min and 1 h of loading relative to FS ($p < 0.0003$, Fig. 6 versus Fig. 5). The 3 kDa dextran reached an equilibrium concentration ratio κ of 0.97 ± 0.08 under SL (Fig. 6), comparable to the value reached under FS. Static loading also significantly reduced the concentration of 70 kDa dextran after 3, 6, 12, 24, and 48 h of loading relative to FS ($p < 0.05$, Fig. 7 versus Fig. 5). The 70 kDa dextran reached a final value of 0.67 ± 0.03 by 24 h of SL (Fig. 7); a concentration ratio that is significantly smaller than that reached after equilibrium under FS ($p < 0.00005$).

Under dynamic loading (DL), the dextran concentration ratio also increased with time for both molecular masses (Fig. 6 and Fig. 7). DL significantly increased the concentration of 3 kDa dextran over SL after 30 min and 1 h of loading ($p < 0.001$). After 24 h of DL, the concentration ratio of 3 kDa dextran reached a comparable level to SL, as demonstrated by an equilibrium value of 1.01 ± 0.03 for DL and 0.97×0.08 under SL (Fig. 6). For 70 kDa dextran, DL significantly increased the solute concentration over SL after

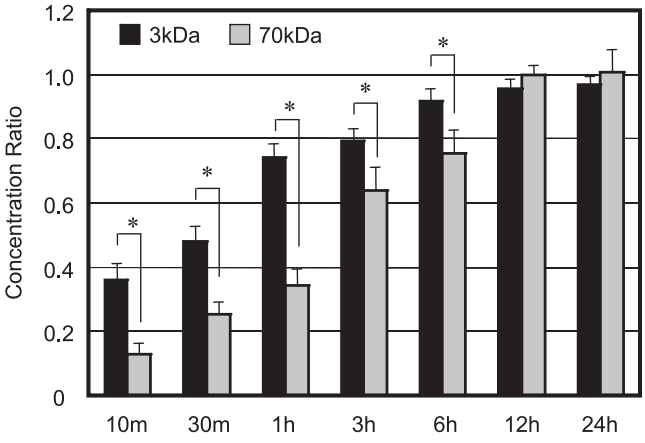

FIGURE 5 Average solute concentration of 3 kDa and 70 kDa dextran measured in Ø5 mm cylindrical disks under free swelling conditions after 10 min, 30 min, 1 h, 3 h, 6 h, 12 h, and 24 h at 37°C. *$p < 0.05$ indicates significance between 3 and 70 kDa dextran.

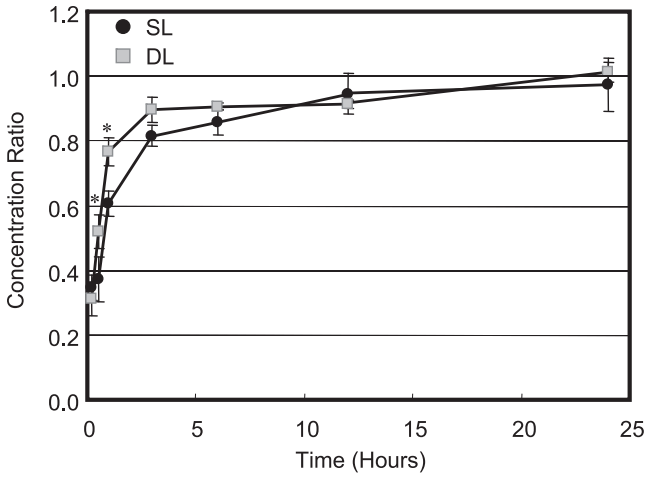

FIGURE 6 Average solute concentration ratio of 3 kDa dextran measured under static (SL) and dynamic (DL) conditions. Concentrations were measured after 10 min, 30 min, 1 h, 3 h, 6 h, 12 h, and 24 h of loading at 37°C. *$p < 0.001$ indicates significance between SL and DL at 30 min and 1 h.

3, 6, 12, and 24 h of loading ($p < 0.001$; Fig. 7). After 24 h of DL, the concentration ratio of 70 kDa reached an equilibrium value of 0.96 ± 0.11, which was significantly greater than that reached under SL (0.67 ± 0.03, $p < 0.001$).

Study 3: strain-dependent solute uptake

The equilibrium solute concentration ratios of 70 kDa dextran, measured at varying magnitudes of compressive strain, are shown in Fig. 8. The concentration ratio was greatest at 0% strain, reaching an average value of approximately unity (0.96 ± 0.11). The application of 5% compressive strain did not result in a marked difference in the equilibrium solute uptake (0.98 ± 0.08, $p > 0.5$). However, the application of 10%, 15%, or 20% compressive strain resulted in a significantly smaller equilibrium solute concentration ratio in comparison to 0% or 5% strain (10%: 0.65 ± 0.07; 15%: 0.63 ± 0.08; and 20%: 0.62 ± 0.04; with $p < 0.005$). No significant difference was found in the concentration ratio among 10%, 15%, and 20% strains (Fig. 8).

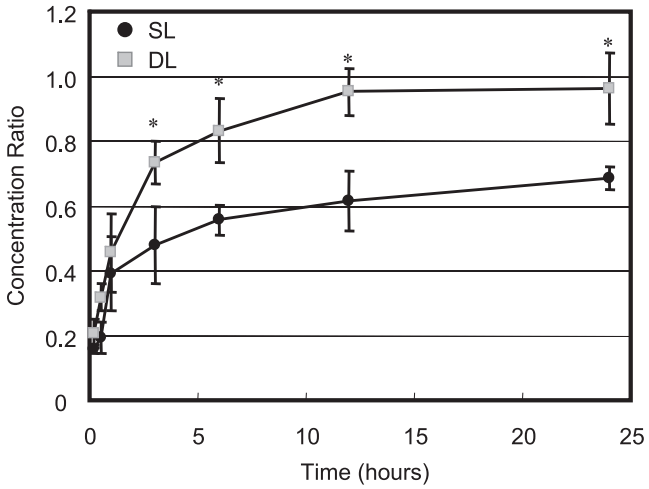

FIGURE 7 Average solute concentration ratio of 70 kDa dextran measured under static (SL) and dynamic (DL) conditions. Concentrations were measured after 10 min, 30 min, 1 h, 3 h, 6 h, 12 h, 24 h, and 48 h of loading at 37°C. *$p < 0.001$ indicates significance between SL and DL at 3, 6, 12, and 24 h.

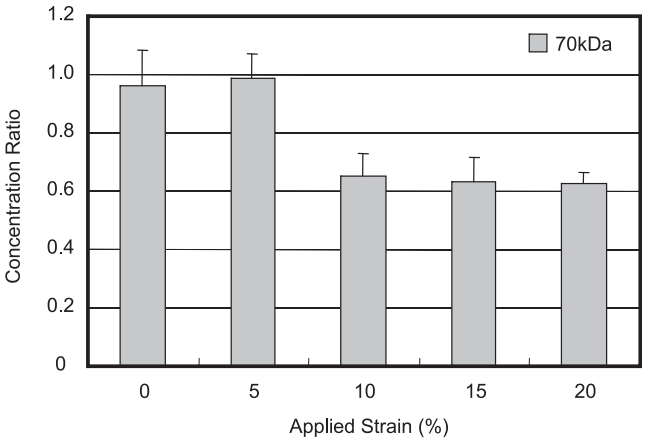

FIGURE 8 Average solute concentration ratio of 70 kDa dextran measured at various compressive strain magnitudes after 48 h of static loading. *$p < 0.001$ indicates significance between lower (0% and 5%) and higher strain magnitudes (10%, 15%, and 20%).

DISCUSSION

The long-term goal of this study is to elucidate the mechanisms influencing matrix elaboration in response to dynamic loading in tissue-engineered constructs. To decouple the effect of mechanotransduction from nutrient transport, this study used a model system of acellular agarose disks and dextran solutions to examine the mechanism of transport in response to loading. Results indicate that dynamic loading significantly enhances the rate of uptake of solutes into agarose disks, as indicated by the slope of solute concentration versus time curves under DL relative to SL (Figs. 6 and 7). Moreover, the enhancement due to dynamic loading was found to be dependent on the molecular weight of the solute. For the larger molecule, the steady-state solute concentration under DL was significantly higher than the corresponding concentration under SL. This finding is the first experimental verification of a nonintuitive active transport phenomenon elucidated in the context of mechanical loading in tissue engineering.

In this study, we examined the effect of DL on 2% agarose hydrogels to mimic the many studies of tissue engineering that utilize agarose as a scaffold for tissue growth. Dextran molecules are extensively used in the study of diffusion and convection in polymeric gels and biological tissues (2,3,11–15). An examination of the passive diffusion response of dextran in agarose demonstrates good agreement with Fick's law of diffusion (Figs. 3 and 4, and Table 1), alleviating potential concerns that the nonglobular morphology

of dextran might produce non-Fickian transport. Dextran molecules, forming polymeric chains, have been shown to exhibit higher diffusivities than expected based on molecular weight predictions (16). Although the results of this study suggest that 70 kDa dextran possesses a comparable diffusivity and partition coefficient to bovine serum albumin (molecular mass: 67 kDa; D: $5.6 - 7 \times 10^{-11}$ m^2/s in agarose), a commonly used spherical solute in transport studies (17), variation in the degree of branching of the molecule may result in a range of diffusivities for different synthesis lots of dextran. Diffusivity measurements using fluorescence recovery after photobleaching have demonstrated the existence of a range of diffusivities for dextran from differing synthetic lots, accounting up to 30–45% variation in the diffusivity. Although this phenomenon may complicate the comparison of results from one study to another, the results reported in this study represent findings from dextran lots with comparable transport behavior. Moreover, tests performed at each time point had agarose disks from a particular casting randomly assigned to each group, limiting any potential bias between the experimental groups.

The transport of solutes in biological tissues is the fundamental process responsible for nutrient supply and waste removal, occurring primarily through either passive diffusion or convective flow. In this study, the uptake of dextran molecules in the FS controls is indicative of the passive diffusion behavior of dextran in agarose gels. The solute concentration of 3 kDa molecules was significantly higher than that of 70 kDa dextran at time points before equilibration (up to 12 h, Fig. 5). This difference in solute uptake is a consequence of differing diffusivities of each molecular-weight (MW) solute, as was determined for transport under SL (Table 1). The decrease in D with increasing MW is consistent with the relationship between solute diffusivity and molecular weight (or size). Additionally, the diffusivities and partition coefficient determined in this study are consistent with literature values determined using other experimental techniques (17,18). After 24 h of FS, the concentration ratio of 3 kDa and 70 kDa reached an equilibrium value of 0.97 ± 0.03 and 1.01 ± 0.08, respectively, representing the partition coefficient of these dextran molecules in 2% agarose (Fig. 5).

Although free swelling and static loading both represent passive diffusion behaviors, the rate of solute uptake is faster under FS than under SL. This is primarily due to the greater fraction of the cylindrical specimen's surface area available for transport and exposed to the surrounding bath under free swelling (circular top surface and cylindrical lateral surface) than under SL (cylindrical lateral surface only). For ∅5 mm disks, 35% of the surface area available for transport under FS is sealed under the application of SL in the unconfined compression configuration. Experimental results confirm this predicted behavior in the case of the smaller molecular mass (3 kDa) as evidenced by the responses in Figs. 5 and 6, which show reduced solute concentration in SL relative to FS at early time points (30 min and 1 h), but not at longer durations. Since the disks reached an equilibrium concentration under SL that is comparable to that at FS, it can be concluded that the static compression did not significantly alter the partition coefficient of 3 kDa dextran (i.e., the total interstitial volume available for 3 kDa solutes).

Static loading also significantly decreased the rate of uptake of 70 kDa dextran in comparison to free swelling ($p < 0.001$). Unlike the 3 kDa case, however, the 70 kDa dextran concentration at 24 h was still significantly lower in SL compared to FS (Fig. 7). Longer applications of SL (up to 48 h) demonstrated that the concentration of 70 kDa dextran does not reach the near-unity values seen under FS. The results of this study suggest that the application of compressive strain decreased the total interstitial volume available for the 70 kDa dextran to occupy under SL compared to FS (Fig. 8). The decrease in equilibrium solute content of 70 kDa dextran at 10% strain compared to 0% strain confirms the notion that static loading results in a constant compaction of pore volume, thus reducing the partition coefficient. Previous studies have also reported a nonunity partition coefficient of bovine serum albumin in 2% agarose, a spherical solute with comparable molecular mass and diffusivity to 70 kDa dextran (17). It should be noted that the dextran partition coefficient in agarose and thus the effect of static strain on solute partitioning is dependent on the many factors governing the agarose microstructure formed during gelation. Studies have shown that gel structural and mechanical properties are dependent on the speed and temperature of cooling during gelation (19).

The presence of dynamic deformational loading resulted in significant enhancement of solute uptake of both 3 kDa (Fig. 6) and 70 kDa dextran (Fig. 7). A comparison between the SL and DL responses, where the loading configurations and surface area available for transport were similar, indicates that DL increased the rate of transport of both MW solutes into the disk, consistent with earlier studies of solute adsorption or desorption under various forms of dynamic loading (4–7). For example, dynamic loading up to 0.1 Hz was shown to increase the desorption of solutes, such as glucose, out of cartilage explants (20).

In addition, DL increased the concentration of 70 kDa dextran by ~50% over SL for all loading durations between 3 and 24 h (Fig. 7). Since the range of compressive strain magnitudes occurring in the SL and DL groups (10–20%) is not associated with strain-dependent solute uptake changes (Fig. 8), the resulting increase in the steady-state solute content represents a transport enhancement mechanism mediated by the dynamic nature of the loading regime. This enhancement of the steady-state concentration under dynamic versus static loading represents an active solute transport mechanism, consistent with our earlier theoretical analysis of solute transport under dynamic loading (21).

The theoretical basis for this observation is that dynamic loading of the gel produces a momentum exchange between

the solid matrix and solute that can pump the solute against its concentration gradient. Taken alone, this mechanism is symmetric (it pumps solute inward during the upstroke, and outward during the downstroke). However, if the solvent exudes from the gel faster than the solute during loading, the relatively greater loss of solvent volume produces a small spike in solute concentration near the periphery. During the upstroke, this local solute concentration is transported inward by the recoiling solid matrix. On the application of the subsequent downstroke this spike is transported outward again, though this time, as it approaches the periphery, it gets strengthened by the repeating pore contraction mechanism. This cycle repeats itself, and as the spike keeps being reinforced near the periphery, the solute penetrates deeper and deeper into the disk, along the radial direction. This mechanism reaches steady state when the concentration inside the disk has elevated sufficiently to balance the inward active pumping process with outward passive diffusion. This study represents the first time that this type of enhancement has been observed experimentally, providing the first evidence in support of that theoretical framework. Based on these results, we have been encouraged to further investigate the theoretical predictions of the model. A study subsequent to the current one has provided additional support for the proposed theoretical framework of enhanced transport under dynamic loading (22). In that study, we first loaded agarose gels dynamically, showing increased dextran uptake relative to the unloaded control group. We subsequently terminated the dynamic loading regime and examined the dextran concentration in those disks that were previously loaded. Over time, the dextran concentration in this treatment group recovered back to the value observed in the unloaded control group, showing that the partition coefficient was not altered by dynamic loading.

According to theory, the extent of solute uptake is dependent on the transport properties of solvent and solute in the mixture. It becomes significant when 1), the solid matrix significantly hinders solute diffusion; 2), the characteristic diffusive velocity of the solvent through the porous matrix is significantly higher than that of the solute; and 3), the characteristic velocity of the solid matrix is significantly greater than the diffusive velocity of the solvent. When these three conditions are met, the rate at which the solute is pumped into the gel exceeds its rate of passive outward diffusion, thus producing a net gain over repetitive cycles of loading. This analysis indicates that the transport behavior may be predicted based on two nondimensional parameters:

- R_d—Representing the ratio of the characteristic gel diffusive velocity of the solute to its ideal characteristic gel diffusive velocity.
- R_g—Representing the ratio of the characteristic diffusive velocity of the solvent in the gel to the characteristic diffusive velocity of the solute in the gel.

For the 70 kDa dextran used in this study, it can be estimated that $R_d \sim 0.8$ and $R_g \sim 20$, which represent the range of parameters under which dynamic loading is predicted to significantly enhance solute transport into the gel. Consequently, all else being equal, larger molecular-weight solutes will exhibit a greater gain than their smaller counterparts, consistent with the experimental findings here.

In functional tissue engineering, the application of dynamic mechanical loading has been shown to lead to enhanced cartilaginous tissue growth relative to FS conditions. Moreover, an earlier study has shown that the stimulatory effect of dynamic loading is synergistically enhanced in the presence of the growth factors IGF-1 (molecular mass = 8 kDa) and TGF-β1 (molecular mass = 25 kDa) (23), as also seen in cartilage explants (7). The results of this study suggest that dynamic physiological deformational loading enhances transport of these growth factors and other cellular nutrients, which may result in significant enhancement in the mechanical properties and matrix elaboration. Additionally, since the solute transport enhancement is time-dependent, dynamic loading protocols may be optimized to increase the net accumulation of nutrients inside the constructs, thus resulting in tissues that are mechanically and chemically stimulated, simultaneously. For example, a previous study examining the effect of duty cycle on tissue growth has shown that continuous dynamic loading for 3 h resulted in better improvement of mechanical properties than three consecutive cycles of 1-hour-on/1-hour-off, when compared to FS controls (24). Increasing the continuous DL duration to 6 and 12 h produced no further improvement, suggesting that nutrient content might have reached saturation levels.

Moreover, as new extracellular matrix is elaborated in the tissue engineered constructs, the effect of dynamic loading on solute transport will become more significant than at the early stages of culture. As the constructs become more and more dense, approaching the density and porosity of native articular cartilage, the theory predicts that dynamic loading will produce significantly greater enhancement of nutrient transport in those conditions than in the early stages of culture. As a consequence, the application of DL for the entire duration of the TE process may be able to supply increased nutrient in the center of the constructs at all stages of growth, than in the limiting factor of passive diffusion alone.

In summary, this study examined the effect of dynamic loading on the uptake of solutes into agarose gels. The results indicated that dynamic loading strongly influences the uptake of solutes into agarose disks, as mediated by a greater rate of transport and increased steady-state solute content, than measured in the absence of loading. The results of this study support the hypothesis that the application of dynamic loading in the presence of growth factors of large molecular weight may result in both a mechanically and chemically stimulating environment for tissue growth. Despite its chainlike morphology, this study confirmed that dextran diffusion follows the Fickian model, therefore supporting its usage as a model solute to study globular mass transport.

This study was funded by the National Institutes of Health (grant Nos. NIAMS AR46532 and AR46568).

REFERENCES

1. McKibbin, B., and A. Maroudas. 1974. Nutrition and metabolism. *In* Adult Articular Cartilage. M. Freeman, editor. Grune & Stratton, New York.
2. Torzilli, P. A., J. M. Arduino, J. D. Gregory, and M. Bansal. 1997. Effect of proteoglycan removal on solute mobility in articular cartilage. *J. Biomech.* 30:895–902.
3. Quinn, T. M., V. Morel, and J. J. Meister. 2001. Static compression of articular cartilage can reduce solute diffusivity and partitioning: implications for the chondrocyte biological response. *J. Biomech.* 34:1463–1469.
4. Quinn, T. M., C. Studer, A. J. Grodzinsky, and J. J. Meister. 2002. Preservation and analysis of nonequilibrium solute concentration distributions within mechanically compressed cartilage explants. *J. Biochem. Biophys. Methods.* 52:83–95.
5. O'Hara, B. P., J. P. Urban, and A. Maroudas. 1990. Influence of cyclic loading on the nutrition of articular cartilage. *Ann. Rheum. Dis.* 49:536–539.
6. Urban, J. P., S. Holm, A. Maroudas, and A. Nachemson. 1982. Nutrition of the intervertebral disc: effect of fluid flow on solute transport. *Clin. Orthop. Relat. Res.* 170:296–302.
7. Bonassar, L. J., A. J. Grodzinsky, E. H. Frank, S. G. Davila, N. R. Bhaktav, et al. 2001. The effect of dynamic compression on the response of articular cartilage to insulin-like growth factor-I. *J. Orthop. Res.* 19:11–17.
8. Mauck, R. L., S. L. Seyhan, G. A. Ateshian, and C. T. Hung. 2002. Influence of seeding density and dynamic deformational loading on the developing structure/function relationships of chondrocyte-seeded agarose hydrogels. *Ann. Biomed. Eng.* 30:1046–1056.
9. Mauck, R. L., M. A. Soltz, C. C. Wang, D. D. Wong, P. H. Chao, et al. 2000. Functional tissue engineering of articular cartilage through dynamic loading of chondrocyte-seeded agarose gels. *J. Biomech. Eng.* 122:252–260.
10. Mauck, R. L., C. C. Wang, E. S. Oswald, G. A. Ateshian, and C. T. Hung. 2003. The role of cell seeding density and nutrient supply for articular cartilage tissue engineering with deformational loading. *Osteoarthritis Cartilage.* 11:879–890.
11. Leddy, H. A., H. A. Awad, and F. Guilak. 2004. Molecular diffusion in tissue-engineered cartilage constructs: effects of scaffold material, time, and culture conditions. *J. Biomed. Mater. Res. B Appl. Biomater.* 70:397–406.
12. Leddy, H. A., and F. Guilak. 2003. Site-specific molecular diffusion in articular cartilage measured using fluorescence recovery after photobleaching. *Ann. Biomed. Eng.* 31:753–760.
13. White, J. A., and W. M. Deen. 2002. Agarose-dextran gels as synthetic analogs of glomerular basement membrane: water permeability. *Biophys. J.* 82:2081–2089.
14. Maroudas, A. 1970. Distribution and diffusion of solutes in articular cartilage. *Biophys. J.* 10:365–379.
15. Kosto, K. B., and W. M. Deen. 2005. Hindered convection of macromolecules in hydrogels. *Biophys. J.* 88:277–286.
16. Deen, W. M. 1987. Hindered transport of large molecules in liquid-filled pores. *Am. Inst. Chem. Eng. J.* 33:1409–1425.
17. Roger, P., C. Mattisson, A. Axelsson, and G. Zacchi. 2000. Use of holographic laser interferometry to study the diffusion of polymers in gels. *Biotechnol. Bioeng.* 69:654–663.
18. Pluen, A., P. A. Netti, R. K. Jain, and D. A. Berk. 1999. Diffusion of macromolecules in agarose gels: comparison of linear and globular configurations. *Biophys. J.* 77:542–552.
19. Aymard, P., D. R. Martin, K. Plucknett, T. J. Foster, A. H. Clark, et al. 2001. Influence of thermal history on the structural and mechanical properties of agarose gels. *Biopolymers.* 59:131–144.
20. Evans, R. C., and T. M. Quinn. 2006. Solute convection in dynamically compressed cartilage. *J. Biomech.* 39:1048–1055.
21. Mauck, R. L., C. T. Hung, and G. A. Ateshian. 2003. Modeling of neutral solute transport in a dynamically loaded porous permeable gel: implications for articular cartilage biosynthesis and tissue engineering. *J. Biomech. Eng.* 125:602–614.
22. Albro, M. A., N. O. Chahine, R. Li, K. Yeager, C. T. Hung, et al. 2008. Dynamic loading of deformable porous media can induce active solute transport. *J. Biomech.* 41:3152–3157.
23. Mauck, R. L., S. B. Nicoll, S. L. Seyhan, G. A. Ateshian, and C. T. Hung. 2003. Synergistic action of growth factors and dynamic loading for articular cartilage tissue engineering. *Tissue Eng.* 9:597–611.
24. Mauck, R. L., C. C.-B. Wang, Q. Cheng, N. Gabriel, E. S. Oswald, et al. 2003. Optimization of parameter for articular cartilage tissue engineering with deformational loading. *In* Transactions of the Orthopedic Research Society. New Orleans, LA. Paper# 0353.